ACS APPLIED MATERIALS & INTERFACES

Research Article

www.acsami.org

Heavily Doped, Charge-Balanced Fluorescent Organic Light-Emitting Diodes from Direct Charge Trapping of Dopants in Emission Layer

Sang Ho Rhee,[†,§] Sung Hyun Kim,[‡,§] Hwang Sik Kim,[†] Jun Young Shin,[†] Jeeban Bastola,[†] and Seung Yoon Ryu*[,†]

[†]Department of Information Communication & Display Engineering, Division of Mechanics and ICT Convergence Engineering, Sunmoon University, 221, Sunmoon-ro, Tangjeong-myeon, Asan, Chungnam 336-708, Republic of Korea

[‡]Department of Chemistry, College of Natural Sciences, Seoul National University, Seoul 151-747, Republic of Korea

Supporting Information

ABSTRACT: We studied the effect of direct charge trapping at different doping concentrations on the device performance in tris(8-hydroxyquinoline) aluminum (Alq_3):10-(2-benzothiazolyl)-2,3,6,7-tetrahydro-1,1,7,7-tetramethyl-1H,5H,11H-(1)-benzopyropyrano(6,7−8-i,j)quinolizin-11-one (C545T) as a host−dopant system of a fluorescent organic light-emitting diode. With increasing C545T doping concentration, trap sites could lead to the promotion of hole injection and the suppression of electron injection due to the electron-transport character of Alq_3 host for each carriers, as confirmed by hole- and electron-only devices. Direct charge injection of hole carriers from the hole transport layer into C545T dopants and the charge trapping of electron carriers are the dominant processes to improve the charge balance and the corresponding efficiency. The shift of the electroluminescence (EL) spectra from 519 nm to 530 nm was confirmed the exciton formation route from Förster energy transfer of host−dopant system to direct charge trapping of dopant-only emitting systems. Variation in the doping concentration dictates the role of the dopant in the fluorescent host−dopant system. Even though concentration quenching in fluorescent dopants is unavoidable, relatively heavy doping is necessary to improve the charge balance and efficiency and to investigate the relationship between direct charge trapping and device performance. Heavy doping at a doping ratio of 6% also generates heavy exciton quenching and excimer exciton, because of the excitons being close enough and dipole−dipole interactions. The optimum device performance was achieved with a 4%-doped device, retaining the high efficiency of 12.5 cd/A from 100 cd/m^2 up to 15 000 cd/m^2.

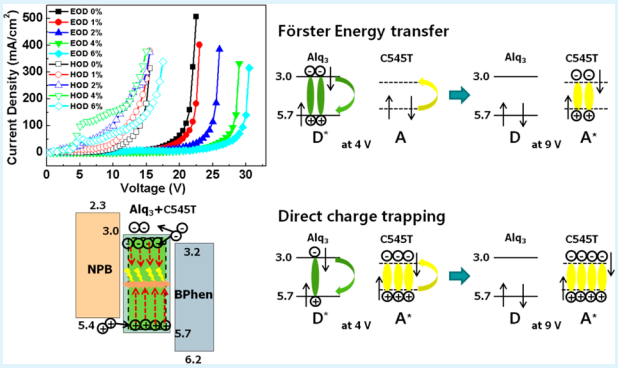

KEYWORDS: *hole/electron injection, fluorescent OLEDs, hole-/electron-only devices, direct charge trapping, trap sites, charge balance*

I. INTRODUCTION

In organic light-emitting diodes (OLEDs), there are two main ways to form excitons. The one way is from Förster energy transfer[1] from host to dopant molecules, and the other one is from direct recombination between holes and electrons at the dopant molecules.[2] The management of doping concentration and energy level alignment through the device structure has been widely developed as an approach to improve device performance, making it possible to lead this technology toward practical applications.[3−6] However, there is still a demand to understand the quantitative contribution in these two light-emission mechanism in terms of singlet excitons formation and quenching, charge injection, charge balance, and so on. This demand is attributed to the benefits of the simple device structure, the exclusion of the costly phosphorescent dopants, and a relatively low fabrication cost.[7−12] Low doping concentration is generally used to obtain the high efficiency of these devices, because its additional loading of dopants gives rise to heavier self-quenching.[10,11] Tris(8-hydroxyquinoline) aluminum (Alq_3):10-(2-benzothiazolyl)-2,3,6,7-tetrahydro-1,1,7,7-tetramethyl-1H,5H,11H-(1)-benzopyropyrano(6,7−8-i,j)quinolizin-11-one (C545T) is the most commonly used host:dopant in green-emitting fluorescent organic light-emitting diodes (FLOLEDs). So far, device performance has been shown to increase the efficiency mainly through control of the thickness and the charge injection/transport capability using by the different energy level layers instead of the commonly used layers in the alternative device structure.[7,13−16] Chwang et al. proposed a graded and mixed stack of an Alq_3:C545T (1 wt %) emitting layer (EML) with hole and electron transport characters, resulting in an efficiency of 10 cd/A at 1000 cd/m^2.[7] Sun et al. obtained a maximum current efficiency of 19.6

Received: May 25, 2015
Accepted: July 7, 2015
Published: July 7, 2015

ACS Publications © 2015 American Chemical Society

DOI: 10.1021/acsami.5b04519
ACS Appl. Mater. Interfaces 2015, 7, 16750−16759

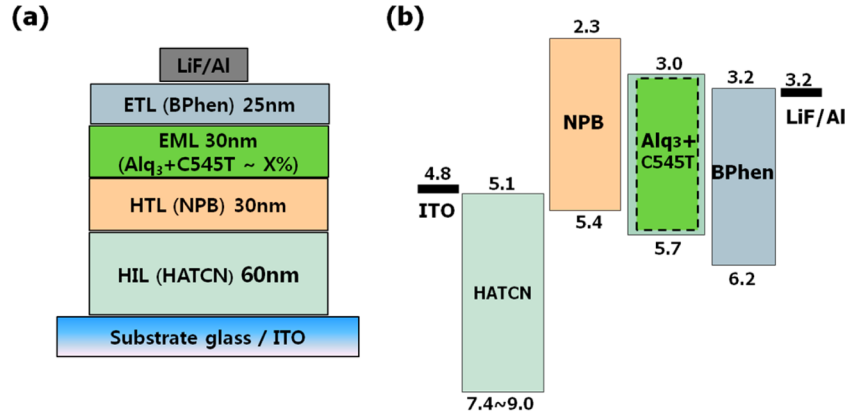

Figure 1. (a) Schematic diagram of device structure of the FLOLEDs for different doping concentrations. (b) Energy level diagram. The band gap difference between Alq_3 and C545T is only ~0.05 eV.

cd/A with an Alq_3:C545T (2 wt %), because of microcavity effects induced by the cathode modification in tandem FLOLEDs.[14] From those approaches, as well as other research reports, the highest current efficiencies were obtained by enhancing Förster energy transfer with low doping concentration of C545T in an Alq_3 host[13−16] and/or by increasing the hole current density via electrode modification.[8−11] Generally, 4%−5% doping in EML has been widely investigated in the case of phosphorescent OLEDs (PHOLEDs) through long-range Dexter energy transfer, compared to low doping (<1%) of FLOEDs with short-range Förster energy transfer by dipole−dipole interaction. In the ideal case, host−guest energy transfer with 1% dopant concentration in PHOLEDs was unusually observed, because of the combination of efficient Förster energy transfer[1] and Dexter energy transfer between host singlet and the metal-to ligand charge-transfer (MLCT) state.[17] That observation means that the conventional concept that heavy doping in PHOLEDs and low doping in FLOLEDs was adopted to increase the efficiency could be reconsidered.

On the other hand, direct charge trapping was developed to increase charge recombination efficiency and to reduce excessive charges for dissipation through the device, which is the primary emission mechanism in highly efficient PHOLEDs with the appropriate doping concentration.[17−20] Heavily doped phosphorescent EML up to 20% without hole injection layer (HIL) and hole transport layer (HTL) were investigated for direct hole injection into triplet dopants.[20] In addition, Liu et al. investigated how the device performance varied with doping concentration up to 23%; the highest efficiency of 14.3 cd/A was obtained for 1% doping of C545T through the modification of the anode with transition metals in FLOLEDs.[13] The current density of the device decreased with increasing doping concentration due to the gradual reduction of current injection capability. They asserted that the high efficiency of 7.5 cd/A in the 4%-doped device originated from the reduction in the current density, compared to the 1% doped device, when a nickel oxide (Ni_2O_3) was used to modify the indium tin oxide (ITO). However, they could not fully investigate the mechanism of efficient device performance, which was originated from direct carrier injection into dopants in EML. It was reported that simply using a metal oxide-modified ITO anode without HIL and HTL was proposed and the current density decreased as the fluorescent doping concentration increased.[13] However, the current density in PHOLEDs was enhanced as the phosphorescent doping concentration was increased in EML in their previous work.[20] In that case, they clearly asserted that the device mechanism for improved devices was direct charge injection into dopants. Regardless, the direct charge trapping mechanism renders the device structure simple and the operating voltage low while maintaining high efficiency. There has been considerable effort in understanding the influence of charge injection/transport and the increased efficiency in Alq_3:C545T host−dopant systems. Nevertheless, a detailed relationship between the contribution of the hole/electron injection and the device performance was not fully investigated, in terms of direct charge trapping with relatively heavy doping in FLOLEDs.

Herein, we simply showed the correlation between direct charge trapping and device performance according to the operating voltage without complicated investigation. The detailed investigation of the contribution between hole and electron injection as a function of the doping concentration was studied by using hole-only/electron-only devices (HODs/EODs) in an Alq_3:C545T host−dopant system of FLOLEDs. A relatively high doping concentration is considered as charge traps at the dopants since the dopant performs the role of charge injection/transport. The optimal doping concentration makes it possible to balance between holes and electrons through direct charge injection, resulting in higher current efficiency, despite heavier self-quenching.

II. EXPERIMENTAL SECTION

The devices were fabricated with a high vacuum (~2×10^{-7} Torr) evaporation process, where constituent organic materials were thermally deposited onto cleaned ITO. For the sample cleaning, the ITO glass was ultrasonically cleaned with acetone and isopropanol (IPA) under sonication at 40 kHz, dipping in boiled IPA, and finally followed by ultraviolet (UV) ozone treatment. The devices were fabricated with a mixture of ITO, 1,4,5,8,9,11-hexaazatriphenylene-hexacarbonitrile (HAT-CN, 60 nm), *N*,*N*-bis(1-naphthyl)-*N*,*N*′-diphenyl-1,1′-biphenyl-4,4′diamine (NPB, 30 nm), Alq_3:C545T (30 nm, *X*%), 2,9-dimethyl-4,7-diphenyl-1,10-phenanthroline (BPhen, 25 nm), LiF(1 nm), and Al (130 nm), in which the doping concentration (*X*) of C545T varied between 0%, 1%, 2%, 4%, and 6% in a high-vacuum chamber. The metal layer was deposited by using a shadow mask with an area of 0.04 cm^2. The thickness of layers was confirmed by spectroscopic ellipsometry (SE). The device structure of the HODs and EODs were constructed as ITO/HATCN(30 nm)/NPB(60 nm)/Alq_3:C545T(60 nm, *X*%)/molybdenum oxide (MoO_3) (10 nm)/Al and ITO/Alq_3:C545T(120 nm, X%)/Bphen(25 nm)/LiF/Al, respectively. The current density−luminance−voltage characteristics and the electroluminescence (EL) spectra of the devices were respectively

DOI: 10.1021/acsami.5b04519
ACS Appl. Mater. Interfaces 2015, 7, 16750−16759

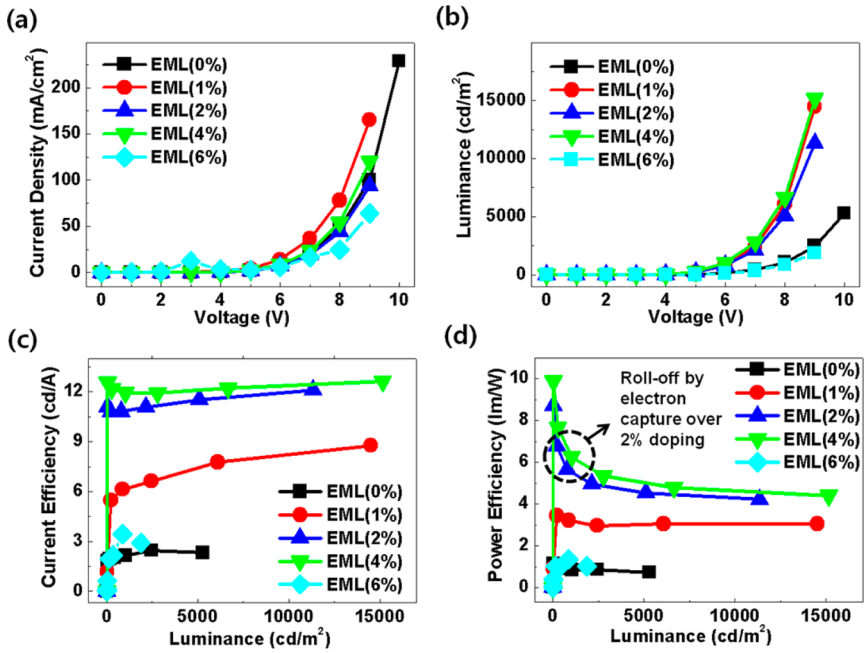

Figure 2. Device performances of the FLOLEDs for different doping concentrations: (a) current density–voltage curves, (b) luminance–voltage curves, (c) current efficiency–luminance curves, and (d) power efficiency–luminance curves. The current efficiency rolloff could be reduced in the 4%-doped device to retain the current efficiency of 12.5 cd/A at 100 cd/m^2 up to 15 000 cd/m^2, while the power efficiency rolloffs for 2%- and 4%-doped device were observed.

obtained using a Keithley Model 2400 voltmeter and a Minolta Model CS-1000 spectrometer, respectively.

III. RESULTS AND DISCUSSION

Figure 1a and 1b show the schematic device structure and energy band diagram of an Alq_3:C545T host–dopant system in a FLOLED, respectively. The EML consists of Alq_3 and C545T, which are an electron-transport-character host material, and a well-known green fluorescent-emitting dopant material, respectively. Excitons generally are formed on the host and are transferred to the dopant through Förster energy transfer process, leading to efficient fluorescence. Based on the device configuration and the energy level diagram, it is assumed that the dopants have a role as trap sites for both electrons and holes, limiting the current density of the devices as the doping concentration increases. In addition to electron-transport character of EML materials, the mobility of electrons in the electron transport layer is faster than that of holes in the hole transport layer ($\mu_{NPB} < \mu_{BPhen}$),[21,22] which electrons can be the main charge carriers in the FLOLEDs. In order to maximize the current efficiency, it is important to enhance charge injection as well as maintain the balance between holes and electrons at the dopants in the EML.[23] Therefore, it can be expected that variations in the doping concentration play a decisive role for charge injection/transport and the corresponding device performance.

Figure 2a depicts the current density–voltage (J–V) curve for different doping concentrations (0%, 1%, 2%, 4%, and 6%). The band-gap difference between Alq_3 and C545T is only ~0.05 eV[24] from both the highest occupied molecular orbital (HOMO) and the lowest unoccupied molecular orbital (LUMO).[24−26] Forsythe et al.[26] reported that the trap energy was adjusted from ~0.25 eV for undoped Alq_3 to ~0.32 eV in Alq_3:C545T, which means that these trap states could be matched with the relative energy level difference between host and guest materials using ultraviolet photoemission spectroscopy (UPS). Electron carriers could be efficiently transferred through host and/or trapped at C545T dopants, whereas hole carriers has the possibility to mostly hop into C545T, because of the electron-transport character of the Alq_3 host.[13,24,25] Moreover, direct hole injection into the dopant is energetically favorable with a barrier lower than 0.3 eV, in terms of the energy level diagram. These assumption suggests that the Alq_3:C545T host–dopant system facilitates the injection of hole carriers directly into the C545T dopants rather than into the Alq_3 hosts. This system renders the electrons also trapped when the host molecules mainly contribute to charge injection.

The device with 1% doping has the highest current density, while the devices with 4%, 2%, and 6% doping show a sequential reduction in current density (Figure 2a). The control device (0% doping of C545T) has a current density similar to that of the device with 2% doping. It was previously predicted that the current density should gradually decrease with increasing doping concentration.[13] However, the current density was found to have a different tendency from the previous prediction. This different tendency may be understood from the different capability of charge injection of holes and electrons into the dopants as the doping concentration changes.

Luminance–voltage (L–V) properties of the devices were investigated for different doping concentrations in Figure 2b. The luminance of all FLOLEDs show similar tendencies to the current densities of the devices, except for the 6%-doped device. The maximal brightness obtained from the 4%-doped device reached up to 15 150 cd/m^2, which is attributed to a higher degree of recombination efficiency of electrons and holes.[27] The turn-on voltage of the doped devices was dropped by increasing the doping concentration, compared to the 0%-doped device. This is confirmed by the fact that the dopants are likely to serve as charge trapping sites for hopping transport. Figure 2c and 2d show current efficiency–luminance and

DOI: 10.1021/acsami.5b04519
ACS Appl. Mater. Interfaces 2015, 7, 16750−16759

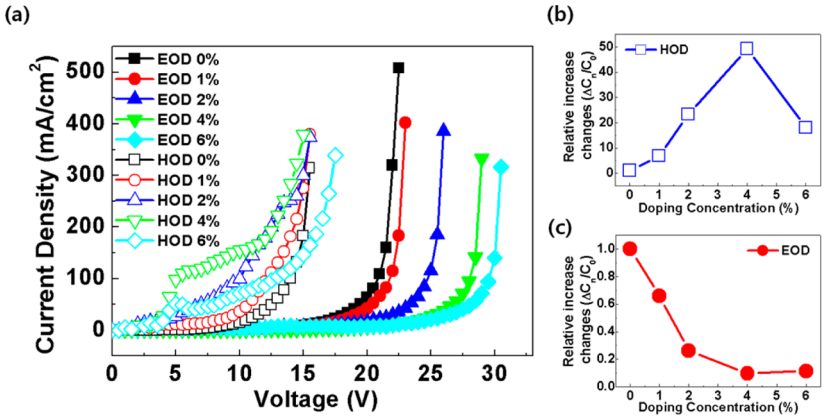

Figure 3. (a) Current density−voltage characteristics of the hole-only and electron-only devices. Relative increase of the current density for different doping concentrations in (b) HODs and (c) EODs. [C_n is the current density of n% doping, and C_0 is the current density of 0% doping.]

power efficiency−luminance of the device with different doping concentrations, respectively. The 4%-doped device exhibited the maximum current efficiency of 12.5 cd/A and 8.5 lm/W at 100 cd/m^2, while the control device with 0% doping concentration had a current density of 1.8 cd/A and 1.1 lm/W at the same luminance. The enhanced current and power efficiency are ascribed to the enhanced hole injection from direct charge trapping, optimizing the charge balance between holes and electrons, and the reduced operation voltage.[28−30] Generally, a higher doping concentration leads to self-quenching because of an increase of dipole−dipole interactions in FLOLEDs, leading to decreased current efficiencies.[11] Although the 4%-doped device induced heavier self-quenching than the 1%-doped device, the charge balance from direct charge injection overcomes the drawback, achieving the highest current efficiency. This coincides with the luminance being the highest in the 4% doped device. The other devices showed much lower current efficiencies, because of charge imbalance. In addition, the current efficiency rolloff could be reduced in the 4%-doped device to retain the current efficiency of 12.5 cd/A at 100 cd/m^2 up to 15 000 cd/m^2, while the power efficiency rolloffs for 2%- and 4%-doped device were observed. The small reduction in current efficiency rolloff might be due to the broad recombination zone as doping concentration increases; however, the power efficiency roll-offs for 2% and 4% doping could be originated from the electron charge carriers' capture at dopant traps as bias is increased. It makes the device operation voltage increased, eventually related to the rolloff of power efficiency, comparing to those of 1%-doped device. The power efficiency rolloff for the 1%-doped device was not observed, which means that carrier capture and increasing operation voltage were insignificant. Both the current and power efficiency for the 6%-doped device show severe exciton quenching. Consequently, direct charge injection of the 4%-doped device readily facilitated exciton formation on dopant molecules, resulting in high efficiency, despite self-quenching.

In order to gain insight into the current densities of the FLOLEDs, the doping dependence of the charge injection capability was investigated by HODs/EODs in Figure 3a. The HODs/EODs indicate change of the current densities according to the applied voltage. The device structure of the HODs and EODs were constructed as ITO/HATCN (30 nm)/NPB (60 nm)/Alq_3:C545T (60 nm, X%)/MoO_3 (10 nm)/Al and ITO/Alq_3:C545T (120 nm, X%)/Bphen (25 nm)/LiF/Al, respectively. The electron injection ability in the EODs was gradually suppressed with increasing doping concentration from 0% to 6%. In this case, the dopant does not favor the injection of electrons into C545T due to the carriers' trap at the dopant site, with respect to the electron-transport character of the Alq_3 host.

The path from the electron transport layer (ETL) to the Alq_3 host and from Alq_3 to the HTL could be preferable for the electron carriers. Some parts of them, naturally, could choose the path from ETL to dopants and from dopants to HTL. However, the dopants could be considered as trap sites, especially for electrons.[13] Thus, the current densities from electron injection in the FLOLEDs were controlled by Schottky barrier and Fowler−Nordheim injection.[31,32] From the standpoint of hole injection, at low operating voltage, the current densities of the HODs showed a drastic increase along with the additional loading of dopants in the host molecules, except for the 6% HOD. We infer that the dopants serve as a hopping site for holes, because of the electron-transport character of Alq_3 host and a lowering of the hole injection barrier, comparing with the electron injection.[17−20] The hole carriers' path from HTL to C545T dopant and from dopant to ETL could be preferable. Some parts of them, possibly, could choose the path from HTL to the Alq_3 host and from the host to ETL. All the HODs approached similar current densities at high operating voltage, illustrating that partly accumulated holes at the interface between the HTL and the EML were also injected into the dopants through the host molecules in addition to direct hole injection. In the case of the 6% HOD, hole leakage might cause a reduction in current density due to doping being large enough to generate deep-trap sites that limit the hole currents, as compared to the shallow traps at lower doping concentrations.[25,32] Therefore, the influence of the different doping concentrations on the HODs/EODs determines the current densities of the FLOLEDs. Direct charge trapping facilitated the hopping of the holes and suppressed electron injection and the electron-transport-character of Alq_3 host for both carriers are quite critical for an injection into the heavily doped EML.

The relative changes ($\Delta C_n/C_0$) of the current densities in the HODs and EODs, compared to the 0% HOD/EOD, as a function of increasing doping concentration, were plotted to investigate the relationship between direct charge trapping and the current density of the FLOLEDs (see Figures 3b and 3c). The driving voltages were set to 8 V for the HODs and to 20 V for the EODs, because the structure of the HOD and EOD was

DOI: 10.1021/acsami.5b04519
ACS Appl. Mater. Interfaces 2015, 7, 16750−16759

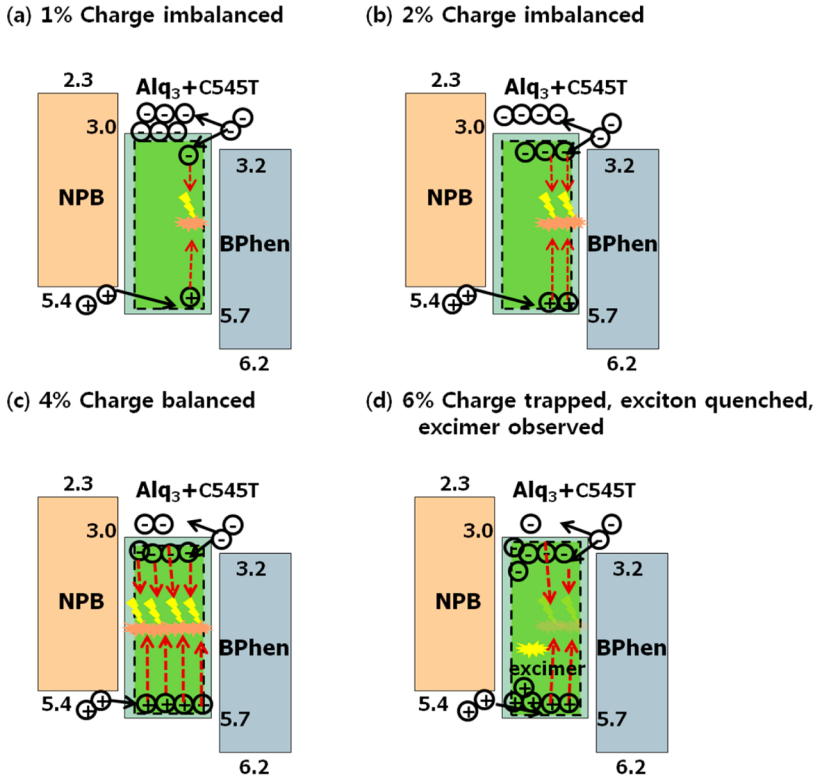

Figure 4. Schematic modeling for different doping (Alq_3 + C545T) concentrations: (a) 1%, (b) 2%, (c) 4%, and (d) 6%.

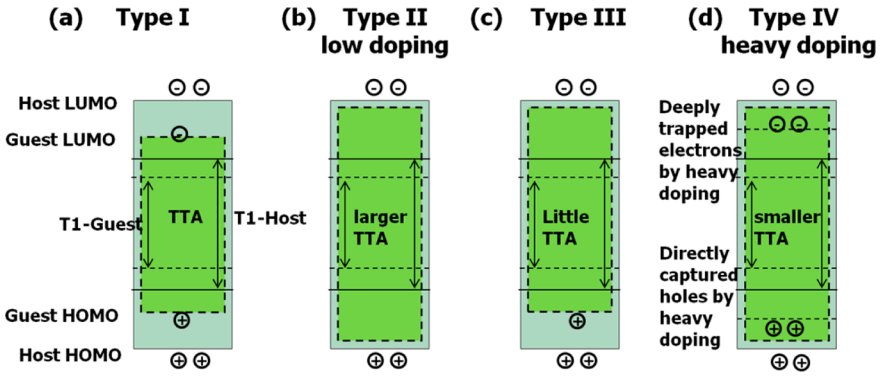

Figure 5. Schematic models to understand the delayed EL by TADF for relatively heavy doping in FLOLED. Delayed EL induced by (a) Type I (large of trapped charges), (b) Type II (small of trapped charges), (c) Type III (mobile electrons and trapped holes charges only), and (d) Type IV (larger of trapped charges).

different in order to prevent a short current circuit. C_n and C_0 denote the current density for n% and 0% doping in the HODs/EODs, respectively. Based on the differences of the current densities in the HODs and the EODs, we illustrated that the current densities in the FLOLEDs are due to discrepancies in the capabilities of hole and electron injection. Basically, the ratio of the increase in HODs and the decrease in EODs caused the different tendency of current densities. Compared to the 0% HOD/EOD, the relative increase of the 1% HOD/EOD was ~6.82 for the HOD and ~0.66 for the EOD, which correlated with the highest current density of the 1%-doped FLOLED among all the FLOLEDs. Even though the relative increase between the 0% and the 2% HOD/EOD were 23.3 for hole injection and 0.26 for electron injection, the current density of the 2%-doped FLOLED was less than that of the 1%-doped FLOLED. This indicates that electron injection is more sensitive than the hole injection, because of the trap sites for the electrons which facilitates relatively more of the electron density in the EML.[33] In the 4% HOD/EOD, electron injection dropped by 1 order of magnitude but hole injection increased remarkably (by ~50 times). This lead to a higher current density in the 4%-doped FLOLED, compared to the 2%-doped FLOLED, because of the direct hole trapping contribution, regardless of the decrease in electron injection. The relative increase in the 6%-doped EOD was similar to the 4%-doped EOD while the 6%-doped HOD showed about a 3-fold decrease. This caused the current density of the 6%-doped FLOLED to be less than that of the 4%-doped FLOLED. From these results, the fluorescent emission mechanism for a given host−dopant system could be shown to be mainly manipulated by direct charge trapping, rather than the commonly proposed Förster energy transfer process.

Schematic modeling corresponding to charge balance and direct charge trapping for both hole's direct injection and

DOI: 10.1021/acsami.5b04519
ACS Appl. Mater. Interfaces 2015, 7, 16750−16759

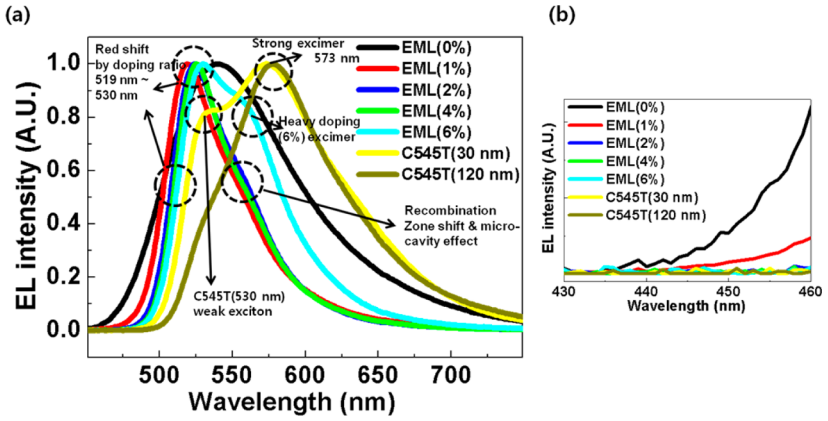

Figure 6. (a) Normalized electroluminescence (EL) spectra of the FLOLEDs for different doping concentrations and C545T EML without Alq_3 from 450 nm to 780 nm. (b) Normalized EL spectra of the FLOLEDs for different doping concentrations and C545T EML without Alq_3 at ∼450 nm.

electron's trapping at C545T dopants are presented in Figure 4. In the case of the 1%-doped device, the hole's direct injection into the dopants is slight, while the electron injection to the host is much greater and the corresponding amount of the electrons at dopant traps are small, because of the electron-transport character of Alq_3 host.[13,24,25] Thus, we expect the highest current density but it induces poor current efficiency, because the electron is the main current flow through the device, in comparison to the number of excitons, which finally decides the current efficiency, as shown in Figure 4a. In the case of the 2%-doped device, there still exists charge imbalance, as shown in Figure 4b; however, the 4%-doped device modeling reveals that the more hole injection occurs at the hopping sites and more electron capture occurs at trap sites, respectively. It eventually facilitates good charge balance in the device and highly efficient FLOLEDs, as shown in Figure 4c. However, the current density of the 6%-doped device are the lowest, because both hole and electron carriers are captured at dopant swallow and deep traps, resulting obviously in the poor current density, HOD/EOD and device performance. Heavy doping also generates heavy exciton quenching and excimer exciton because of close enough among excitons and dipole−dipole interaction as shown in Figure 4d.[11]

Triplet−triplet annihilation (TTA) or triplet-polaron annihilation (TPA) by heavy doping are totally different from those by light doping, in terms of thermally activated delayed fluorescence (TADF).[34−36] Luo and Aziz[24] suggested three types of host−guest systems with low doping ratio, in terms of the delayed EL. Type I has the captured holes and electrons kept at guest trap sites by relative large energy barriers between host and guest materials, indicating that TTA is slightly affected in delayed EL, as shown in Figure 5a. In the case of Type II, the reduced energy barrier between the host and guest materials leads to the decrease of trapped charges as well as the increase of TTA. Thus, the delayed EL is revealed by mainly the TTA process, such as an Alq_3:C545T system with low doping ratio (1%), as shown in Figure 5b. In the case of Type III, only holes are captured at guest sites through the large energy barriers of the HOMO between the host and the guest, providing that TTA does not strongly contribute to the delayed EL. In this work, Alq_3:C545T system with relatively heavy doping ratio (over 2%) could show a different trend, compared to Types I, II, and III. On the basis of this trend, we suggest a new modeling (we denoted as Type IV) in Figure 5d. Even though there is a small energy barrier between host and guest materials, unlikely to the Type II for the energy level alignment, the large amount carriers was trapped due to relatively heavy doping. As a result, delayed EL could be reduced by the decrease of TTA process. It can be good agreement with the current density investigation in which we proposed the charge transport of holes and electrons. Namely, the holes were directly captured while electrons were trapped deeply in the Alq_3:C545T system with relatively heavy doping of dopants.

Figure 6a shows the normalized electroluminescence (EL) spectra of doped FLOLEDs for different doping concentrations. Without doping C545T, the peak at 550 nm was assigned to the pristine Alq_3. Similar EL spectra of the doped devices were observed with the green emission; the main peak changed from 519 nm to 530 nm by changing the doping ratio coincident with the previous works for the Alq_3:C545T host−dopant system.[13] In OLEDs, there are two common reasons responsible for the blue-shift in device emission color with varying current/voltage. The first one might be attributed to the generation of high-energy excitons under higher applied voltage.[37] This type of blue-shift is common in mostly all white OLEDs and even in some single-color emission devices fabricated by coevaporation of host and dopant materials due to a strong solid-state solvation effect.[38,39] The amount of the color shift can be practically reduced by changing the doping concentration. The second is the fact that the recombination zone in the devices can be relocated by the redistribution of the charge carriers due to the change of applied voltage.[40] The Commission Internationale de l'Eclairage (CIE) color coordinates for doping concentrations of 0%, 1%, 2%, 4%, and 6% are (0.381, 0.560), (0.290, 0.640), (0.305, 0.650), (0.309, 0.650), and (0.366, 0.608), respectively. The maximum peak position was shifted to longer wavelengths with increasing doping concentration, corresponding to the *x*-color coordinate shift from 0.290 to 0.366, as shown in Figure S1 in the Supporting Information. This is consistent with other reports that the formation of excimers facilitates a bathochromic shift and broad spectrum of the EL emissions.[13,41,42] Another possibility could be that the route for exciton generation was changed from Förster energy transfer to direct charge trapping at the dopants. To verify these assumptions, the exciton formation investigation between host−dopant systems and dopant-only systems is needed (*vide infra* in Figure 3). Microcavity effect from different recombination zone shift

DOI: 10.1021/acsami.5b04519
ACS Appl. Mater. Interfaces 2015, 7, 16750−16759

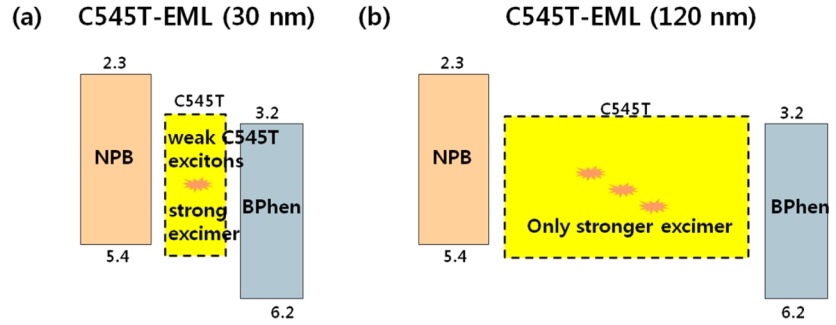

Figure 7. Schematic modeling for C545T EML without Alq_3: (a) 30 nm EML and (b) 120 nm EML.

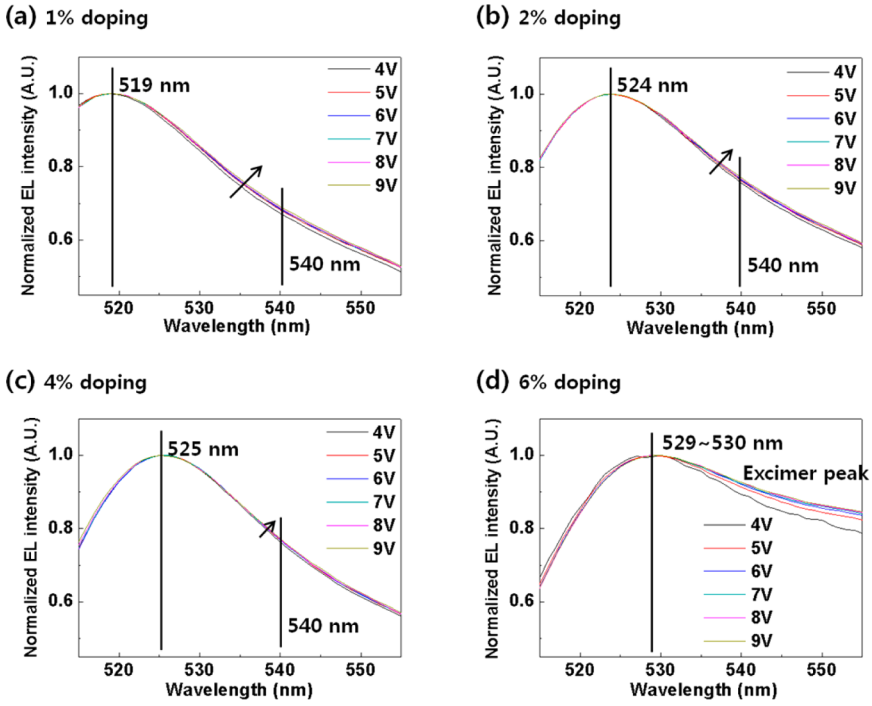

Figure 8. Normalized electroluminescence spectra of the FLOLEDs for different doping concentrations by doping ratio and operating voltage from 510 nm to 560 nm: (a) 1% doping, (b) 2% doping, (c) 4% doping, and (d) 6% doping.

from 1%-, 2%-, and 4%-doped devices could be also possible to explain the marginal shoulder peak's shift at ~550 nm. The strong shoulder peak of the 6%-doped device was reported as a weak excimer emission at previous work due to the C545T's heavy doping.[13]

To correlate C545T only in EML and excimer-emission peak in detail, the two devices using only C545T EML (30 and 120 nm) without Alq_3 in EML were fabricated as shown in Figure S2 in the Supporting Information. The device performances such as current density−voltage, luminance−voltage, current efficiency−luminance, and power efficiency−luminance curves of the FLOLEDs for different doping concentrations and C545T only without Alq_3 in EML have been presented in Figure S3 in the Supporting Information. Even though the potential barriers in LUMO between NPB and C545T and in HOMO between C545T and BPhen do exist, the 30 nm thickness of C545T in the device showed low operation voltage, which could be ascribed to the quasi-ohmic contact between NPB and C545T and between C545T and BPhen. The 120 nm C545T in the device showed high operation voltage, because of thicker EML. However, both devices of 30 and 120 nm of the EML showed poor efficiencies, because of the severe quenching like the 6%-doped device in the Alq_3 host, that is, the excessive increase in the concentration of the dopants gives rise to heavier self-quenching.[10,11] Note that all current and power efficiencies of the 0%- and 6%-doped devices with the C545T dopant and the device with only C545T in the EML (30 and 120 nm) were almost similar.

The EL peaks of the device with C545T only in the EML are also shown in Figure 6a; the main peak positions were observed at ~573 nm and showed a broad spectrum. There is almost no overlap between the emission and absorption, which was confirmed as excimer formation by C545T.[13,41,42] In the case of a 30 nm thickness of C545T in the EML, 530 and 573 nm of the spectra were originated from C545T exciton and strong excimer-emission, respectively. EL spectra of the host−dopant (Alq_3 + C545T) devices were observed with the green emission ranging from 519 nm to 530 nm through the change in doping ratio. It means that exciton formation route could be changed from the Förster energy transfer in the 1%-doped device into direct charge trapping mechanism over 2%-doped devices. However, in the case of 120 nm C545T in the EML, only a stronger excimer peak at ~573 nm was observed. It can be assigned based on the fact that the amount of excimer excitons

DOI: 10.1021/acsami.5b04519
ACS Appl. Mater. Interfaces 2015, 7, 16750−16759

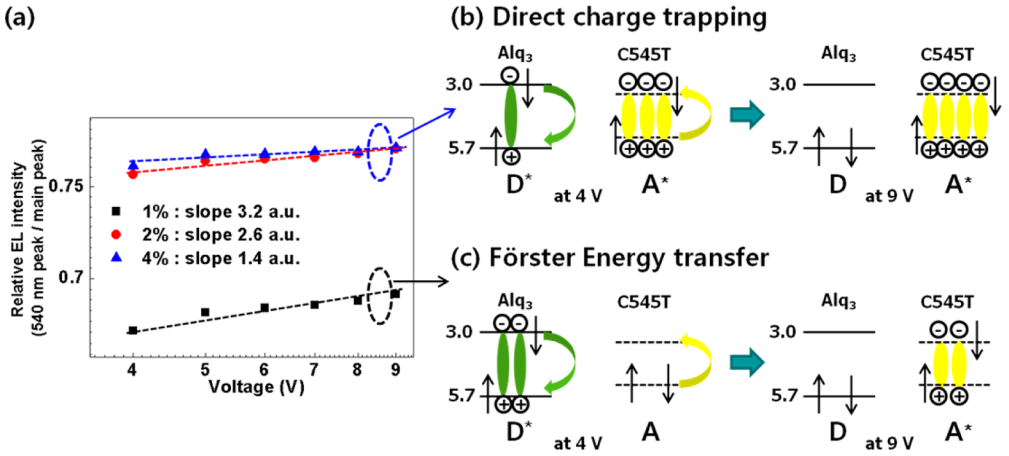

Figure 9. (a) Relative EL intensity, which is defined as the relative ratio between the peak at ~540 nm and the main peaks of doped devices, according to the operation voltage of 1%, 2%, 4% doping (a.u. means arbitrary unit). Schematic modeling for (b) direct charge trapping and (c) Förster energy transfer.

is dependent on the thickness of the EML, as shown in Figure 7. Generally, excimer emission is strongly dependent on chemical intermolecular structure, physical doping concentration, and charge transport properties, affecting the recombination characteristics in the emissive region.[41,42] The sole C545T for EML affected the different recombination mechanism from a thickness between 30 nm and 120 nm, because of the difference in the mobility between holes and electrons. In thicker layers of C545T (120 nm), discrepant carrier mobility between them could strongly stimulate the generation of excimer emission, while reducing the amount of pure excitons of C545T. Those excimer emissions from C545T showed the yellowish color with CIE color coordinates of (0.460, 0.527) for 30 nm and (0.495, 0.499) for 120 nm, as shown in Figure S1 in the Supporting Information. For the much thicker EML, the CIE color coordinate was shifted to yellow and reddish.[13,41,42]

Normalized EL intensities by doping ratio, according to the operating voltage (from 4 V to 9 V), are shown in Figure 8. The main peak of 1%, 2%, 4%, and 6% doping were 519, 524, 525, and 529 nm, respectively. Moreover, the EL intensities of 540 nm shoulder peaks were increased as the operating voltage was increased, as shown in Figure 8, which means the route of exciton formation were changed. The shoulder peak of the 1%-doped device between 530 nm and 540 nm was strengthened according to the operation voltage increase from 4 V to 9 V, while that of the 4%-doped device was almost unchanged. That could be attributed to that the exciton formation route in 1%-doped device has been changed, while that of 4%-doped device was stable, even at high operation voltage. In addition, the band gap difference between Alq_3 and C545T is only ~0.05 eV,[24−26] which corresponds the wavelength difference between Alq_3 + C545T from Förster energy transfer for 1% exciton doping and C545T direct charge trapping for over 2% exciton doping to ~10 nm. It can be calculated by the equation of $E = hc/\lambda$, where E is a photon energy, h is Plank's constant, c is the velocity of light, and λ is the wavelength. This calculation is exactly coincident with the experiment result from the main peak of 1% doping to that of 6% doping, which means the exciton formation route was totally converted from the Förster energy transfer for 1% doping device to direct charge trapping for over 2% doping devices, as shown in Figures 9a and 9b. The relative ratio of EL intensity between the peaks at ~540 nm and the main peaks of doped devices (from 1% to 6% doping), according to the operation voltage, is presented in Figure 9a. With 6% doping in the host, the shoulder peak was observed as excimer emission.[13] The detailed change of C545T exciton formation at 530 nm is shown in Figure S4 in the Supporting Information and the relationship between the doping ratio and the operating voltage have been presented as Figure S5 in the Supporting Information. The EL intensities of C545T exciton at 530 nm increased as the doping ratio was increased, which is attributed to the change of the exciton formation route. For underlying exciton formation mechanism, Förster energy transfer was converted to direct charge trapping in the change of doping concentration from 1% over 2%.

In addition, the slight peak at ~455 nm in the 0%- and 1%-doped devices was assigned to NPB emission.[43,44] There were no blue emission in 2%-, 4%-, and 6%-doped devices and the C545T EML devices as shown in Figure 6b, respectively. The NPB emission might be due to charge leakage from the EML and the recombination between overflowed electrons and accumulated holes at the interface of HTL and EML. The discrepancy between the current density and the efficiency can be explained by the NPB emission when the EL emission intensity is proportional to the exciton density in EML. Even though the 1% doped device showed higher EL emission intensity, compared with the 2%-doped device, the current efficiency of the 1%-doped device was less than that of the 2%-doped device, because of NPB emission, as shown in Figure S6 in the Supporting Information. In addition, the 4%-doped device showed the highest EL intensity without charge leakage, which is consistent with the current efficiency data. The heavier self-quenching facilitates the relatively low EL intensity of the 6%-doped device, because of nonradiative recombination. From the investigation of EL spectra, it is evident that the recombination zone is delocalized with increasing doping concentration and is confined to the EML. The lifetime of the devices with different doping concentrations (0%, 1%, 2%, 4%, and 6%) at the initial luminescence of 1000 cd/m^2 without getter was investigated as shown in Figure S7 in the Supporting Information. The tendency of lifetime data simply followed the trend in the current efficiency of the devices. The lifetimes of devices with 2 and 4% doping were similar to each other and superior to those of other devices. However, the lifetime of the

DOI: 10.1021/acsami.5b04519
ACS Appl. Mater. Interfaces 2015, 7, 16750−16759

device with 6% doping presented the most severe degradation, because of TTA and TPA quenching.

IV. CONCLUSION

We investigated the detailed correlation between direct charge trapping and device performance, depending on the doping concentration in an Alq_3:C545T host−dopant system by the quantitative comparison of injection contribution from hole and electron carriers. The hole injection capability was strengthened, whereas the electron injection ability was suppressed as doping concentration was increased, because of the electron-transport character of the Alq_3 host. Direct charge trapping was found to be the main operating mechanism, which is responsible for enhancing device performance. The 10 nm red-shifts of EL spectra provide the change of exciton formation route from Förster energy transfer of the host−dopant system to direct charge trapping of a dopant-only emitting system.

In addition to the charge injection investigation, the EL emission intensity of the FLOLEDs confirmed the corresponding recombination efficiency between holes and electrons. An excimer emission from 6%-doped device was also observed in shoulder peak, identified by the EL with a configuration of the device using only C545T in EML. As a result, we obtained highly efficient green FLOLEDs with relatively high doping concentrations (4%) of C545T. The efficient charge balance at dopants was obtained by direct charge trapping, resulting from the ideal contribution of hole and electron injection, regardless of unavoidable self-quenching.

■ ASSOCIATED CONTENT

Supporting Information

The CIE color coordinates of various devices of the FLOLEDs for different doping concentrations and C545T EML without Alq_3 are shown in Figure S1. A schematic diagram and an energy level diagram of the device structure of C545T EML without Alq_3 are shown in Figure S2. Device performances (current density−voltage curves, luminance−voltage curve, current efficiency−luminance curve and power efficiency−luminance curve) are presented in detail in Figure S3. The detailed change of C545T exciton formation at 530 nm is shown in Figure S4, and the relationship between the doping ratio and the operating voltage are presented as Figure S5. Electroluminescence spectra of the FLOLEDs without normalization for different doping concentrations are shown in Figure S6. The lifetime of the devices with different doping concentrations (0%, 1%, 2%, 4%, and 6%) at the initial luminescence of 1000 cd/m^2 without getter is added as Figure S7. The Supporting Information is available free of charge on the ACS Publications website at DOI: 10.1021/acsami.5b04519.

■ AUTHOR INFORMATION

Corresponding Author

*Tel.: +82-41-530-2295. E-mail: justie74@sunmoon.ac.kr.

Author Contributions

[§]These authors are equally contributed to this paper. The manuscript was written through contributions of all authors. All authors have given approval to the final version of the manuscript.

Notes

The authors declare no competing financial interest.

■ ACKNOWLEDGMENTS

This research was supported by Basic Science Research Program through the National Research Foundation of Korea (NRF) funded by the Ministry of Education (Nos. 2014R1A1A2059762 and 2011-0014497) and the Industrial Strategic Technology Development Program, No. 10042412) funded by the Ministry of Knowledge Economy (MKE, Korea). Following are results of a study on the "Leaders in Industry−University Cooperation" Project, supported by the Ministry of Education, Science & Technology (MEST).

■ REFERENCES

(1) Förster, T. 10th Spiers Memorial Lecture. Transfer Mechanisms of Electronic Excitation. *Discuss. Faraday Soc.* **1959**, *27*, 7−17.
(2) Utsugi, K.; Takano, S. Luminescent Properties of Doped Organic EL Diodes Using Naphtalimide Derivative. *J. Electrochem. Soc.* **1992**, *139*, 3610−3615.
(3) Tang, C. W.; Vanslyke, S. A. Organic Electroluminescent Diodes. *Appl. Phys. Lett.* **1987**, *51*, 913−915.
(4) Tang, C. W.; Vanslyke, S. A.; Chen, C. H. Electroluminescence of Doped Organic Thin Films. *J. Appl. Phys.* **1989**, *65*, 3610−3616.
(5) Zhou, L. S.; Wanga, A.; Wu, S. C.; Sun, J.; Park, S. K.; Jackson, T. N. All-Organic Active Matrix Flexible Display. *Appl. Phys. Lett.* **2006**, *88*, 083502-1−083502-3.
(6) So, F.; Kido, J.; Burrows, P. Organic Light-Emitting Devices for Solid-State Lighting. *MRS Bull.* **2008**, *33*, 663−669.
(7) Chwang, A. B.; Kwong, R. C.; Brown, J. J. Graded Mixed-Layer Organic Light-Emitting Devices. *Appl. Phys. Lett.* **2002**, *80*, 725−727.
(8) Hu, W. P.; Matsumura, M. Organic Single-Layer Electroluminescent Devices Fabricated on CuOx-Coated Indium Tin Oxide Substrate. *Appl. Phys. Lett.* **2002**, *81*, 806−807.
(9) Chan, I. M.; Hsu, T. Y.; Hong, F. C. Enhanced Hole Injections in Organic Light-Emitting Devices by Depositing Nickel Oxide on Indium Tin Oxide Anode. *Appl. Phys. Lett.* **2002**, *81*, 1899−1901.
(10) Lane, P. A.; Kushto, G. P.; Kafafi, Z. H. Efficient, Single-Layer Molecular Organic Light-Emitting Diodes. *Appl. Phys. Lett.* **2007**, *90*, 023511-1−023511-3.
(11) Tse, S. C.; Tsung, K. K.; So, S. K. Single-Layer Organic Light-Emitting Diodes Using Naphthyl Diamine. *Appl. Phys. Lett.* **2007**, *90*, 213502-1−213502-3.
(12) Chan, I. M.; Hong, F. C. Improved Performance of the Single-Layer and Double-Layer Organic Light Emitting Diodes by Nickel Oxide Coated Indium Tin Oxide Anode. *Thin Solid Films* **2004**, *450*, 304−311.
(13) Liu, Z.; Helander, M. G.; Wang, Z.; Lu, Z. Efficient Single-Layer Organic Light-Emitting Diodes Based on C545T−Alq_3 System. *J. Phys. Chem. C* **2010**, *114*, 11931−11935.
(14) Sun, J. X.; Zhu, X. L.; Peng, H. J.; Wong, M.; Kwok, H. S. Effective Intermediate Layers for Highly Efficient Stacked Organic Light-Emitting Devices. *Appl. Phys. Lett.* **2005**, *87*, 093504-1−093504-3.
(15) You, H.; Dai, Y.; Zhang, Z.; Ma, D. Improved Performances of Organic Light-Emitting Diodes with Metal Oxide as Anode Buffer. *J. Appl. Phys.* **2007**, *101*, 026105-1−026105-3.
(16) Chu, T. Y.; Chen, J.-F.; Chen, S.-Y.; Chen, C.-J.; Chen, C. H. Highly Efficient and Stable Inverted Bottom-Emission Organic Light Emitting Devices. *Appl. Phys. Lett.* **2006**, *89*, 053503-1−053503-3.
(17) Jeon, W. S.; Park, T. J.; Kim, S. Y.; Pode, R.; Jang, J.; Kwon, J. H. Ideal Host and Guest System in Phosphorescent OLEDs. *Org. Electron.* **2009**, *10*, 240−246.
(18) Gong, X.; Ostrowski, J. C.; Moses, D.; Bazan, G. C.; Heeger, A. J. Electrophosphorescence from a Polymer Guest-Host System with an Iridium Complex as Guest: Förster Energy Transfer and Charge Trapping. *Adv. Funct. Mater.* **2003**, *13*, 439−444.
(19) Lv, Y.; Zhou, P.; Wei, N.; Peng, K.; Yu, J.; Wei, B.; Wang, Z.; Li, C. Improved Hole-Transporting Properties of Ir Complex-Doped

Organic Layer for High-Efficiency Organic Light-Emitting Diodes. *Org. Electron.* **2013**, *14*, 124−130.
(20) Liu, Z. W.; Helander, M. G.; Wang, Z. B.; Lu, Z. H. Efficient Bilayer Phosphorescent Organic Light-Emitting Diodes: Direct Hole Injection into Triplet Dopants. *Appl. Phys. Lett.* **2009**, *94*, 113305-1−113305-3.
(21) Naka, S.; Okada, H.; Onnagawa, H.; Yamaguchi, Y.; Tsutsui, T. Carrier Transport Properties of Organic Materials for EL Device Operation. *Synth. Met.* **2000**, *111-112*, 331−333.
(22) Naka, S.; Okada, H.; Onnagawa, H.; Tsutsui, T. High Electron Mobility in Bathophenanthroline. *Appl. Phys. Lett.* **2000**, *76*, 197−199.
(23) Kim, S. H.; Jang, J. S.; Hong, J.-M.; Lee, J. Y. High Efficiency Phosphorescent Organic Light Emitting Diodes Using Triplet Quantum Well Structure. *Appl. Phys. Lett.* **2007**, *90*, 173501-1−173501-3.
(24) Luo, Y.; Aziz, H. Correlation Between Triplet−Triplet Annihilation and Electroluminescence Efficiency in Doped Fluorescent Organic Light-Emitting Devices. *Adv. Funct. Mater.* **2010**, *20*, 1285−1293.
(25) Luo, Y.; Aziz, H.; Popovic, Z. D.; Xu, G. Electric-Field-Induced Fluorescence Quenching in Dye-Doped Tris(8-hydroxyquinoline) Aluminum Layers. *Appl. Phys. Lett.* **2006**, *89*, 103505-1−103505-3.
(26) Forsythe, W.; Morton, D. C.; Le, Q. T.; Yan, L.; Nuesch, F.; Tang, C. W.; Gao, Y. Energy Alignment and Trap States in Dye Doped tris-8-(hydroxyquinoline) Aluminum Light-Emitting Devices. *Proc. SPIE* **1999**, *3623*, 13−19.10.1117/12.348397
(27) Kim, S. H.; Jang, J. S.; Yook, K. S.; Lee, J. Y. Stable Efficiency Roll-Off in Phosphorescent Organic Light-Emitting Diodes. *Appl. Phys. Lett.* **2008**, *92*, 023513-1−023513-3.
(28) He, G. F.; Pfeiffer, M.; Leo, K.; Hofmann, M.; Birnstock, J.; Pudzich, R.; Salbeck, J. High-Efficiency and Low-Voltage p i n Electrophosphorescent Organic Light-Emitting Diodes with Double-Emission Layers. *Appl. Phys. Lett.* **2004**, *85*, 3911−3913.
(29) He, G. F.; Schneider, O.; Qin, D. S.; Zhou, X.; Pfeiffer, M.; Leo, K. Very High-Efficiency and Low Voltage Phosphorescent Organic Light-Emitting Diodes Based on a p-i-n Junction. *J. Appl. Phys.* **2004**, *95*, 5773−5777.
(30) Kim, S. H.; Jang, J. S.; Yook, K. S.; Lee, J. Y.; Gong, M.-S.; Ryu, S. O.; Chang, G.-K.; Chang, H. J. Triplet Host Engineering for Triplet Exciton Management in Phosphorescent Organic Light-Emitting Diodes. *J. Appl. Phys.* **2008**, *103*, 054502-1−054502-4.
(31) Burrows, P. E.; Shen, Z.; Bulovic, V.; McCarty, D. M.; Forrest, S. R.; Cronin, J. A.; Thompson, M. E. Relationship between Electroluminescence and Current Transport in Organic Heterojunction Light-Emitting Devices. *J. Appl. Phys.* **1996**, *79*, 7991−8006.
(32) Parker, I. D. Carrier Tunneling and Device Characteristics in Polymer Light-Emitting Diodes. *J. Appl. Phys.* **1994**, *75*, 1656−1666.
(33) Murata, H.; Merritt, C. D.; Kafafi, Z. H. Emission Mechanism in Rubrene-Doped Molecular Organic Light-Emitting Diodes: Direct Carrier Recombination at Luminescent Centers. *IEEE J. Sel. Top. Quantum Electron.* **1998**, *4*, 119−124.
(34) Uoyama, H.; Goushi, K.; Shizu, K.; Nomura, H.; Adachi, C. Highly Efficient Organic Light-Emitting Diodes from Delayed Fluorescence. *Nature* **2012**, *492*, 234−238.
(35) Hirata, S.; Sakai, Y.; Masui, K.; Tanaka, H.; Lee, S. Y.; Nomura, H.; Nakamura, N.; Yasumatsu, M.; Nakanotani, H.; Zhang, Q.; Shizu, K.; Miyazaki, H.; Adachi, C. Highly Efficient Electroluminescence Based on Thermally Activated Delayed Fluorescence. *Nat. Mater.* **2014**, *14*, 330−336.
(36) Song, D.; Wang, Q.; Zhao, S.; Aziz, H. Dependence of Carrier Recombination Mechanism on the Thickness of the Emission Layer in Green Phosphorescent Organic Light-Emitting Diodes. *Org. Electron.* **2011**, *12*, 582−588.
(37) Shao, Y.; Yang, Y. White Organic Light-Emitting Diodes Prepared by a Fused Organic Solid Solution Method. *Appl. Phys. Lett.* **2005**, *86*, 073510-1−073510-3.
(38) Jou, J.; Chiu, Y.; Wang, C.; Wang, R.; Hu, H. Efficient, Color-Stable Fluorescent White Organic Light-Emitting Diodes with Single Emission Layer by Vapor Deposition from Solvent Premixed Deposition Source. *Appl. Phys. Lett.* **2006**, *88*, 193501-1−193501-3.
(39) Bulovic, V.; Deshpande, R.; Thompson, M. E.; Forrest, S. R. Tuning the Color Emission of Thin Film Molecular Organic Light Emitting Devices by the Solid State Solvent Effect. *Chem. Phys. Lett.* **1999**, *308*, 317−322.
(40) Tutiŝ, E.; Berner, D.; Zuppiroli, L. Internal Electric Field and Charge Distribution in Multilayer Organic Light-Emitting Diodes. *J. Appl. Phys.* **2003**, *93*, 4594−4602.
(41) Hu, J.-Y.; Pu, Y.-J.; Nakata, G.; Kawata, S.; Sasabe, H.; Kido, J. A Single-Molecule Excimer-Emitting Compound for Highly Efficient Fluorescent Organic Light-Emitting Devices. *Chem. Commun.* **2012**, *48*, 8434−8436.
(42) Williams, E. L.; Haavisto, K.; Li, J.; Jabbour, G. E. Excimer-Based White Phosphorescent Organic Light Emitting Diodes with Nearly 100% Internal Quantum Efficiency. *Adv. Mater.* **2007**, *19*, 197−202.
(43) Ikai, M.; Tokito, S.; Sakamoto, Y.; Suzuki, T.; Taga, Y. Highly Efficient Phosphorescence from Organic Light-Emitting Devices with an Exciton-Block Layer. *Appl. Phys. Lett.* **2001**, *79*, 156−158.
(44) Kim, S. H.; Jang, J.; Lee, J. Y. High Efficiency Phosphorescent Organic Light-Emitting Diodes Using Carbazole-Type Triplet Exciton Blocking Layer. *Appl. Phys. Lett.* **2007**, *90*, 223505-1−223505-3.

NOTE ADDED AFTER ASAP PUBLICATION

This paper was published ASAP on July 21, 2015, with an error to Figure 5's caption. The corrected version reposted on July 21, 2015.

DOI: 10.1021/acsami.5b04519
ACS Appl. Mater. Interfaces 2015, 7, 16750−16759